

Optical properties of patterned InAs quantum dot ensembles grown on GaAs nanopiramids

B. L. Liang,^{a)} P. S. Wong, N. Nuntawong, A. R. Albrecht, J. Tatebayashi, T. J. Rotter, G. Balakrishnan, and D. L. Huffaker^{b)}

Center for High Technology Materials, University of New Mexico, Albuquerque, New Mexico 87106, USA

(Received 29 August 2007; accepted 13 November 2007; published online 11 December 2007)

We demonstrate the ability to form either coupled or isolated patterned quantum dot (PQD) ensembles on nanopatterned GaAs pyramidal buffers. The coupled PQD “clusters” consist of close-spaced PQDs with inter-QD spacing of 5 nm. The isolated PQD “pairs” are comprised of two PQDs well separated by 110 nm. The photoluminescence behavior, measured in integrated intensity, linewidth, and emission peak as a function of excitation intensity and temperature, indicates lateral coupling within the QD clusters and an isolated nature for QD pairs. The ability to tailor PQD formation and subsequent carrier recombination characteristic may prove useful in developing PQD-based devices for optical computing applications. © 2007 American Institute of Physics.

[DOI: 10.1063/1.2821121]

Semiconductor quantum dots (QDs) are subject of interest because of their potential in optoelectronic device applications.^{1–4} Currently, the most common semiconductor QD formation technique involves strain-driven self-assembly by molecular beam epitaxy or metal-organic chemical-vapor deposition (MOCVD) known as the Stranski-Krastanov (SK) growth mode. However, the stochastic nature of SK growth results in a random QD distribution in size and location, along with a residual wetting layer, which presents an obstacle for many applications.^{5–7} Several alternative approaches to QD formation using strain engineering and selective area epitaxy have been studied in an attempt to avoid these problems.^{8–11} Our group has recently explored the nucleation of InAs QDs on a nanofaceted GaAs pyramidal buffer grown on a patterned substrate.^{12–14} High quality patterned QDs (PQDs) featuring room-temperature photoluminescence (PL) and electroluminescence have been demonstrated.^{14,15} Our research reveals that the PQD nucleation depends strongly on the faceted nature of the GaAs pyramid and results in the formation of QD clusters, pairs, or single QDs. In this work, we investigate the optical and structural characteristics of the InAs PQD clusters and pairs grown on faceted GaAs pyramidal buffers.

The samples were grown in a low-pressure (60 torr) vertical Thomas-Swan MOCVD reactor with trimethylgallium, trimethylindium, and tertiarybutylarsine on a GaAs (100) substrate with a 25 nm thick SiO₂ pattern. The pattern was a two-dimensional array of circular holes, 230 nm (\pm 10 nm) in diameter with a pitch of 330 nm created by interferometric lithography and dry etching. The highly faceted pyramidal buffers were formed under specific growth conditions to realize a distinct equilibrium crystal shape (ECS) limited by high index {115}, {105}, {113}, {103}, and (001) facets. The ECS formation, growth conditions, and their effect on PQD nucleation were described in Refs. 12 and 13. After the growth of the pyramidal buffer, the substrate temperature was reduced to 510 °C for the deposition of 2 ML InAs forming PQDs on the GaAs pyramids. The nature of the

PQD ensemble (cluster or pair) depended on the nanofacets of the GaAs pyramid and can be explained by the minimization of QD energy,^{12,14} leading to close-spaced QD clusters of sample A or separated QD pairs of sample B. The PQD ensembles were characterized by *ex situ* high resolution scanning electron microscopy (HR-SEM) analysis. For PL investigation, the PQDs were capped with 20 nm GaAs grown at 510 °C. The samples were mounted on the cold finger of a closed-cycle cryostat (8–300 K). An excitation laser, operating at 785 nm, was focused on the sample surface to a spot size of \sim 100 μ m diameter. The PL signal was dispersed by a monochromator and then detected by an In-GAs detector.

The HR-SEM images of the distinctly different PQDs in samples A and B are shown in Figs. 1(a)–1(f). Figure 1(a) shows a large array of similar PQD clusters of sample A on the patterned substrate. A higher resolution image [Fig. 1(b)] reveals an average of six QDs per GaAs pyramid. These PQDs form two cluster groups and each cluster includes approximately three QDs nucleated on the (115) facets,¹² although clusters with two or four QDs are also observed. The QDs in each cluster are close grouped with a tip-to-tip separation of 45 nm and a base-to-base distance of 5 nm. The QD height varies from 10.2 to 17 nm, as shown by the height profiles in Fig. 1(c). Sample B, shown in Figs. 1(d)–1(f), features one pair of PQDs per pyramid which preferentially nucleate on the (113) facet.¹² The QD pair on each pyramid is separated by 110 nm base-to-base distance. The PQD has a base diameter of 40 nm and a height of about 19 nm.

The PL spectra for sample A and sample B are measured at low temperature (8 K) with a low excitation intensity of 0.06 W/cm². We estimate this pump intensity to provide about one carrier per 100 QDs, assuming that every excitation photon can generate one carrier and the average lifetime of photon-excited carriers is 1 ns.¹⁶ Thus, only the ground state of the QDs is excited. As shown in Fig. 2, sample A exhibits a PL peak at 1.049 eV with a linewidth [full width at half maximum (FWHM)] of 88 meV. This PL peak is asymmetric with a prominence on the higher energy side, which originates from small QDs and reflects the nonuniform size distribution of the PQD clusters. In comparison with sample A, sample B has a narrower PL FWHM of 54 meV due to

^{a)}Electronic mail: bliang@chtm.unm.edu

^{b)}Also at Electrical Engineering Department, University of California at Los Angeles, Los Angeles, CA 90095. Electronic mail: huffaker@ee.ucla.edu

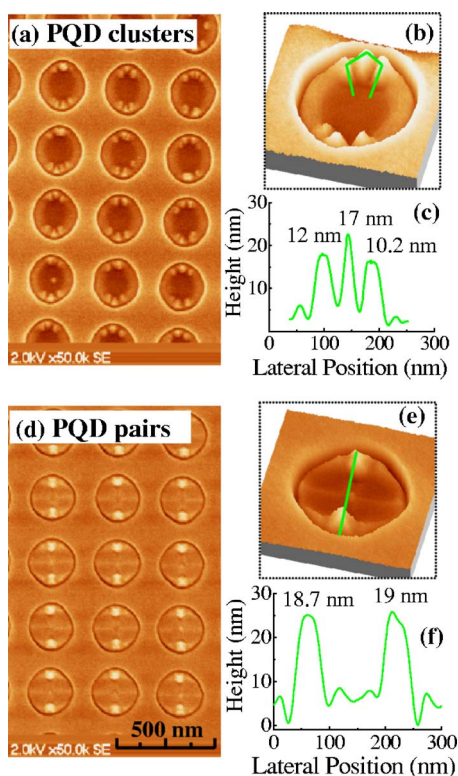


FIG. 1. (Color online) (a) SEM image of the PQR clusters of sample A. (b) Higher resolution SEM image of PQRs on single pyramid. (c) Height profile of one PQR cluster, as shown in (b). (d) SEM image of the PQR pairs of sample B. (e) Higher resolution SEM image of one PQR pair on single pyramid. (f) Height profile of the PQR pair, as shown in (d).

the more uniform QD size distribution and a redshifted PL peak at 0.985 eV due to the larger QD height.

The PL properties, including integrated intensity and FWHM, are examined as a function of the excitation laser intensity at a low temperature of 8 K. Integrated PL intensities are plotted in Fig. 3(a) for both samples. Over a wide range of excitation intensity (0.02–10 W/cm²), the data can be fit to a linear function suggesting that the patterned InAs QDs have a very good crystal quality and the carrier losses due to nonradiative recombination are small.¹⁷ At higher excitation intensity >10 W/cm², the radiative recombination of carriers from the ground states of QDs is saturated and results in a reduced slope in the integrated intensity plot as seen by other researchers.¹⁸

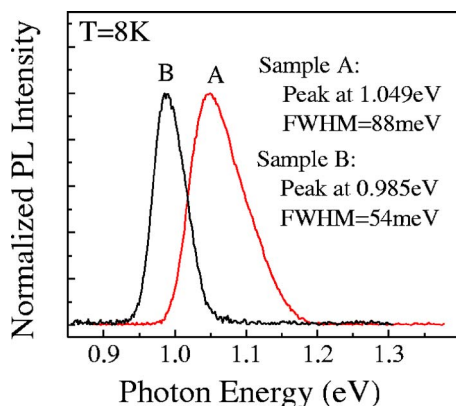


FIG. 2. (Color online) Low temperature ($T=8$ K) PL spectra obtained with a laser excitation intensity of 0.06 W/cm² for samples A and B.

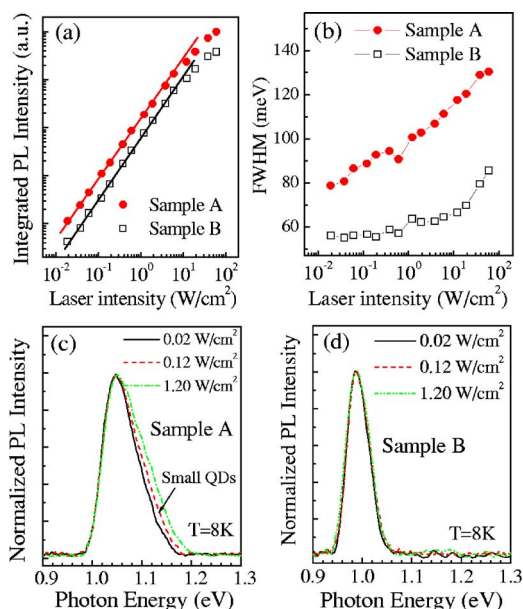


FIG. 3. (Color online) (a) Integrated PL intensity as a function of excitation intensity. The solid lines are linear fitting results. (b) PL FWHM as a function of excitation intensity. (As it is always in this paper, the lines that connected the experimental data points are added only for the guidance of eyes.). Spectra profile as a function of excitation intensity for (c) sample A and (d) sample B.

Figure 3(b) shows the dependence of PL FWHM on the laser excitation intensity. Interestingly, even at low pump intensity, the two samples behave differently. For sample A, the FWHM increases from 79 to 111 meV as the excitation intensity is increased from 0.02 to 10 W/cm². However, for sample B, the FWHM only slightly changes in the low excitation intensity regime and it begins to rapidly increase after the ground PL recombination is saturated at the laser excitation intensity of 10 W/cm². We attribute the FWHM behavior with excitation intensity in sample A to carrier transfer between the laterally coupled PQRs. The photon-excited carriers transfer via tunneling from small QDs to large QDs filling the large QDs first. However, as the excitation laser intensity increases, the probability of the carrier recombination in small QDs increases as large QDs are filled. Therefore, we observe the FWHM increasing even before the appearance of excited state emission.

To verify this hypothesis, the PL spectral profiles are also analyzed. For this analysis, the excitation intensity is kept lower than 1.2 W/cm² to avoid excited state occupation and emission. Figure 3(c) shows the normalized PL spectra for sample A. The FWHM and spectral profile are sensitive to the excitation intensity; we notice a clear broadening at the high-energy side of the PL band corresponding to small QD emission. This can be regarded as an indication of carrier tunneling processes from small QDs to large QDs due to quantum coupling among QD clusters. Such PQR clusters with lateral coupling could act as a “QD molecule,” which is interesting for performing complex quantum computing operations.^{19–21} Figure 3(d) shows the normalized PL spectra for sample B. No broadening or profile changing is observed as the excitation intensity increases from 0.02 to 1.2 W/cm², which demonstrates that there is no carrier tunneling in each QD pair for sample B due to the large separation between the two QDs.

Figure 4 shows the temperature dependence of PL parameters. The excitation laser intensity is set to 2 W/cm² in

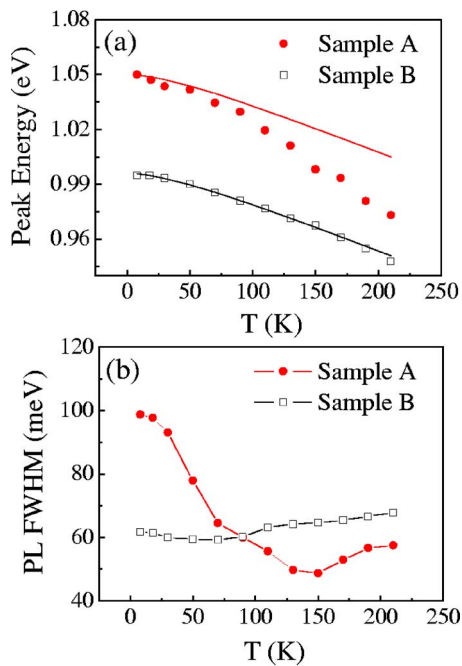


FIG. 4. (Color online) (a) PL Peak energy as a function of temperature, the solid curves are the fitting results according to Varshni law. (b) PL FWHM as a function of temperature.

the low excitation regime. The PL peak position is plotted in Fig. 4(a), where the solid curves are calculated according to the Varshni law²² using parameters of bulk InAs. For sample B, the redshift of the PL peak position with temperature agrees very well with the change of the InAs band gap, which means that sample B has a relatively uniform QD size distribution and its PL peak shift is mainly caused by the variation of InAs band gap. Sample A, however, is characterized by two regimes. Below 50 K, the PL peak does not shift much with temperature. Perhaps below this temperature, excitons occupy the QDs statistically and can only transfer between them by carrier tunneling since their thermal energy is too small. Above 50 K, the PL peak is much more sensitive to changes in temperature. In this scenario, carriers redistribute themselves thermally over the entire QD population and thermalize to the large QD ground states.

Additional information on the carrier transfer can be extracted from the temperature dependence of FWHM shown in Fig. 4(b). For sample A at 8 K, excitons statistically occupy the QDs and the FWHM obtains a maximum value of 99 meV due to the nonuniform QD size distribution. The FWHM then decreases with increasing temperature. At 150 K, the FWHM reaches the minimum of 48 meV, about half of its maximum value at 8 K. This is a typical characteristic of InAs QD ensembles and the reduction of FWHM is generally attributed to the carrier thermal redistribution among the QDs.²³ However, the measured FWHM of our PQD clusters decreases continuously from the low temperature of 8 K. This behavior is different compared to SK QDs, in which the FWHM generally starts to decrease at higher temperature (~ 80 K) due to carrier thermal activation.^{18,23}

Our data indicate again that in this low temperature regime, there is substantial QD-QD carrier transfer via tunneling. In comparison with sample A, sample B exhibits a small FWHM variation of only a few meV in the temperature

range from 8 to above 200 K, which signifies high uniformity and thermally isolated nature of the QDs.

In conclusion, we demonstrate PQD ensembles formed controllably atop GaAs pyramidal buffers with both coupled (clusters) and isolated (pairs) characteristics. The linear dependence of the integrated PL intensity on the excitation intensity signifies a very good crystalline quality for both quantum structures. The QD clusters show a rapid increase in the ground state PL FWHM under low excitation conditions, whereas the QD pairs do not. The ground state PL linewidth of the QD clusters shrinks by 52% (51 meV) as the temperature increases from 8 to 150 K. These observations indicate a lateral coupling between neighboring QDs for QD clusters but none for the QD pairs. Both coupled and isolated QD ensembles have applications in future device technology.

The authors gratefully acknowledge the financial support of the NSF of IGERT through DGE-0504276 and DARPA through HR 0011-05-1-0006.

¹M. Bayer, P. Hawrylak, K. Hinzer, S. Fafard, M. Korkusinski, Z. R. Wasilewski, O. Stern, and A. Forchel, *Science* **291**, 451 (2001).

²Z. Yuan, B. E. Kardynal, R. M. Stevenson, A. J. Shields, C. J. Lobo, K. Cooper, N. S. Beattie, D. A. Ritchie, and M. Pepper, *Science* **295**, 102 (2002).

³X. Q. Li, Y. W. Wu, D. Steel, D. Gammon, T. H. Stievater, D. S. Katzer, D. Park, C. Piermarocchi, and L. J. Sham, *Science* **301**, 809 (2003).

⁴E. A. Stinaff, M. Scheibner, A. S. Bracker, I. V. Ponomarev, V. L. Korenev, M. E. Ware, M. F. Doty, T. L. Reinecke, and D. Gammon, *Science* **311**, 636 (2006).

⁵Q. Xie, A. Madhukar, P. Chen, and N. P. Kobayashi, *Phys. Rev. Lett.* **75**, 2542 (1995).

⁶D. Bimberg, M. Grundmann, and N. N. Ledentsov, *Quantum Dot Heterostructures* (Wiley, New York, 1998).

⁷S. Kiravittaya, A. Rastelli, and O. G. Schmidt, *Appl. Phys. Lett.* **87**, 243112 (2005).

⁸S. Kohmoto, H. Nakamura, T. Ishikawa, and K. Asakawa, *Appl. Phys. Lett.* **75**, 3488 (1999).

⁹M. H. Baier, S. Watanabe, E. Pelucchi, and E. Kapon, *Appl. Phys. Lett.* **84**, 1943 (2004).

¹⁰J. Martin-Sanchez, Y. Gonzalez, L. Gonzalez, M. Tello, R. Garcia, D. Granados, J. M. Garcia, and F. Briones, *J. Cryst. Growth* **284**, 313 (2005).

¹¹B. L. Liang, Zh. M. Wang, J. H. Lee, K. A. Sablon, Yu. I. Mazur, and G. J. Salamo, *Appl. Phys. Lett.* **89**, 043113 (2006).

¹²P. S. Wong, G. Balakrishnan, N. Nuntawong, J. Tatebayashi, and D. L. Huffaker, *Appl. Phys. Lett.* **90**, 183103 (2007).

¹³S. Birudavolu, N. Nuntawong, G. Balakrishnan, Y. C. Xin, S. Huang, S. C. Lee, S. R. J. Brueck, C. P. Hains, and D. L. Huffaker, *Appl. Phys. Lett.* **85**, 2337 (2004).

¹⁴D. L. Huffaker, C. P. Hains, N. Nuntawong, Y. C. Xin, P. S. Wong, L. Xue, S. R. J. Brueck, and L. Lester, *J. Appl. Phys.* **99**, 033503 (2006).

¹⁵P. S. Wong, J. Tatebayashi, B. L. Liang, N. Nuntawong, M. N. Kutty, and D. L. Huffaker, "Electroluminescence Characteristics of Broad-Area LEDs Based on Patterned Quantum Dots by MOCVD" (to be published).

¹⁶S. Lan, K. Akahane, H. Z. Song, Y. Okada, M. Kawabe, T. Nishimura, and O. Wada, *Phys. Rev. B* **61**, 16847 (2000).

¹⁷S. Martini, A. A. Quivy, A. Tabata, and J. R. Leite, *J. Appl. Phys.* **90**, 2280 (2001).

¹⁸J. W. Tomm, T. Elsaesser, Yu. I. Mazur, H. Kissel, G. G. Tarasov, Z. Ya. Zhuchenko, and W. T. Masselink, *Phys. Rev. B* **67**, 045326 (2003).

¹⁹S. Surapapich, S. Thainoi, S. Kanjanachuchai, and S. Panyakeow, *J. Vac. Sci. Technol. B* **23**, 1217 (2005).

²⁰V. Lippen, R. Nötzel, G. J. Hamhuis, and J. H. Wolter, *J. Appl. Phys.* **97**, 044301 (2005).

²¹S. Kiravittaya, R. Songmuang, A. Rastelli, H. Heidemeyer, and O. G. Schmidt, "Multi-scale ordering of self-assembled InAs/GaAs(001) quantum dots," *Nanoscale Research Letters* **1**, 1 (2006).

²²K. P. O' Donnell and X. Chen, *Appl. Phys. Lett.* **58**, 2914 (1991).

²³D. I. Lubyshv, P. P. Gonzalez-Borrero, E. Marega, Jr., E. Petitprez, N. La Scala, Jr., and P. Basmaji, *Appl. Phys. Lett.* **68**, 205 (1996).